Advanced Engineering Informatics 46 (2020) 101161

Contents lists available at ScienceDirect

Advanced Engineering Informatics

journal homepage: www.elsevier.com/locate/aei

Augmenting a deep-learning algorithm with canal inspection knowledge for reliable water leak detection from multispectral satellite images

Jiawei Chen[a], Pingbo Tang[b,*], Todd Rakstad[c], Michael Patrick[c], Xiran Zhou[d]

[a] Del E. Webb School of Construction, Arizona State University, Tempe, AZ, United States
[b] Department of Civil and Environmental Engineering, Carnegie Mellon University, Pittsburgh, PA, United States
[c] Salt River Project Corporation, Tempe, AZ, United States
[d] China University of Mining and Technology, Xuzhou, Jiangsu, China

ARTICLE INFO

Keywords:
Multispectral satellite image
Deep learning
Physics-guided neural network
Convolutional neural network
Landsat 8

ABSTRACT

Maintenance planning of groundwater delivery infrastructure, such as canals, requires labor-intensive field inspection for properly allocating maintenance resources to sections of water infrastructure based on their deterioration conditions. Defective canal sections have cracks where the water delivery performance degrades. In practice, canals can be tens or even hundreds of miles long. Manual canal inspections could take weeks, while could hardly achieve comprehensive water leakage assessment. Another difficulty is that most cracks are developing under the water. Without drying up the canals, inspectors could not observe underwater conditions. They would have to assess visible parts of water facilities and environments (e.g., humidity changes and vegetation growths nearby) for prioritizing canal sections in terms of leaking risks. Even experienced inspectors need much time to complete a reliable canal condition assessment.

This paper presents a deep-learning approach augmented by canal inspection knowledge to achieve automated and reliable water leak detection of canal sections from Landsat 8 satellite images. Such integration utilizes the domain knowledge of experienced inspectors in augmenting the deep-learning methods for more reliable image pattern classification that supports rapid canal condition assessment. Compared with machine learning algorithms trained by raw satellite images manually labeled as leaking, domain-knowledge-augmented deep learning algorithms use satellite image augmented by pixel-level land surface temperature (LST), fractional vegetation coverage (FVC) and Temperature Vegetation Dryness Index (TVDI) as training samples. Specifically, LST, FVC, and TVDI for each pixel are physical parameters derived from Landsat 8 satellite images by remote sensing methods. The “leaking” or “no-leaking” labels of the training samples are from the concrete surface inspection records collected during annual dry-ups of the canal from 2016 to 2019. Testing results on data sets collected for canals flowing through both urban and rural areas show that the proposed approach can achieve recall at 86%, precision at 86%, and accuracy at 85%. The precision, recall, and accuracy of the proposed approach are similar to a conventional deep learning algorithm that uses raw images for training while being more computationally efficient. The reason is that the new approach only processes three channels rather than the 11 channels in raw images. The authors also tested how different combinations of environmental features influence the performance of the algorithm. The results showed that two feature combinations: (LST, FVC) and (LST, FVC, TVDI) achieve the most robust performance in diverse geospatial environments.

1. Introduction

Significant water losses from irrigation canals can result in problems in water conservation, soil erosion, waterlogging, and salinity [16]. Numerous irrigation districts in western states of the US are losing significant amounts of water from canals due to water leakage [1]. Lining a canal with an impermeable concrete layer could help reduce water losses. The United States Bureau of Reclamation reported that seepage could be reduced from 50% or more for earthen canals to 10% for concrete-lined canals [18]. A canal liner, in conjunction with a concrete cover, can further reduce that seepage to less than 5%.

One problem of lined canals is that concrete deterioration could produce water leaks. Harsh environmental conditions can erode concrete structures and canal linings [18] and result in water damages and

* Corresponding author.
E-mail address: ptang@andrew.cmu.edu (P. Tang).

https://doi.org/10.1016/j.aei.2020.101161
Received 16 March 2020; Received in revised form 13 July 2020; Accepted 20 August 2020
Available online 02 September 2020

leaks. Effective monitoring and routine maintenance or repair on concrete structures and canal linings are thus paramount to keep water facilities in acceptable conditions. Moreover, early identification of concrete deteriorations of canals could prevent expensive repairs or replacement of concrete linings later.

Concrete deterioration assessment of canals and water leak analysis also has significant socio-economic impacts. Irrigation canals have been used for centuries to transport water to crops [2]. The irrigation canal system plays a critical role in making the metropolitan area a livable community. For example, as the national oldest multipurpose water reclamation project, the Salt River Project (SRP) operates and maintains an irrigation system that typically delivers more than 325 million gallons of water to municipal, industrial, agricultural, and urban irrigation systems annually [21]. Each fall and winter, SRP personnel spend around two months to perform maintenance to reduce seepage on selected sections of the 131-mile canal network in Phoenix [21]. The selection of the canal sections requires inspectors to assess the deterioration trends of the concrete lining of canals for effective maintenance planning.

The current approach of canal inspection often involves manual inspection with limited technologies for detailed and objective condition assessments. In many cases, even spending hours in the field, inspectors could still miss defects and could hardly measure sediments and defects hidden under the water or buried in the soil. According to the manual of *Canal Operation and Maintenance: Concrete Lining and Structures* by US Department of the Interior, Bureau of Reclamation [11], establishing a formal inspection program is vital to maintaining the condition of concrete structures and canal linings. Inspectors must identify and assess the signs of the surface damages meticulously. Specifically, the challenge of canal condition assessment lies in the tedious canal condition assessments that mostly produce field notes that are subjective and could hardly support reliable deterioration trend analysis of concrete lining.

In recent years, remote sensing techniques are showing the potential of achieving economic, fast, and precise water leakage detection. For example, satellite images and 2D/3D imaging techniques have been attracting the practitioners for improved efficiency and effectiveness of the inspection of water infrastructure [7]. Previous research explored various methods for detecting water leakage through measuring pressure and flow rate changes [24], analyzing acoustic signals of running water [9], and using radar to detect the soil moisture [10]. Remote sensing techniques, such as ground and satellite image analyses, could automate the assessment of the conditions of civil infrastructures [3,7]. A few challenges make these remote sensing techniques impractical: 1) **Visibility challenge** - most of them need direct observations of concrete and cannot assess underwater conditions; 2) **Extensibility challenge** - certain remote sensing and pattern classification algorithms developed for certain regions could hardly work for other regions; 3) **Reliability challenge** – most machine learning algorithms published achieved high precisions and recalls in relatively simple environments (e.g., leaks in the middle of a desert), but the performance on satellite images collected from diverse environments (e.g., urban areas) are either not published or significantly weaker than simple contexts.

This research aims at addressing the challenges mentioned above through a deep-learning approach augmented by domain knowledge about particular physical parameter spatiotemporal patterns that possibly reflect leaks. For example, thermal dynamics knowledge about how water penetration influences the temperature distributions around leaking canals could guide engineers to find leaks. Machine learning approaches augmented by such physics-based knowledge are "*Physics-based learning methods*." Some researchers augmented artificial neural networks, a type of machine learning methods, with physics-based domain knowledge, and call such techniques as "Physics-Guided Neural Networks" or PGNN [13]. Unlike the conventional "black-box" neural networks, this PGNN approach could help researchers examine and explain how different environmental conditions influence the performance of the developed machine learning models in leak detection. Specifically, the authors expect that the PGNN approach could achieve improved precision and recall rates in water leak detection on satellite images collected from diverse geospatial environments. With that in mind, the researchers established a computational framework to validate the performance of a PGNN approach in water leak detection based on satellite images.

Compared with machine learning algorithms trained by labeled raw satellite image samples, the new deep learning algorithms augmented by canal inspection knowledge can use satellite images augmented by pixel-level land surface temperature (LST), fractional vegetation coverage (FVC) and Temperature Vegetation Dryness Index (TVDI) as training samples of leaking and non-leaking canal sections. More specifically, LST, FVC, and TVDI for each pixel are physical parameters derived from Landsat 8 satellite images by remote sensing algorithms. Literature review results and domain knowledge of canal inspectors both indicate that specific patterns of these physical parameters can serve as reliable indicators of water leaks. The proposed method uses the augmented satellite image samples with pixel-level LST, FVC, and TVDI values to train a deep learning network for classifying leaking and no-leaking sections of canals. The researchers collected leakage data of canal systems in Arizona, the US from the year 2016–2018 annually to test the developed methodology in both urban and rural contexts. The collected data included the geolocations of the canal leakage and Landsat 8 multispectral satellite images. Furthermore, the authors explored different combinations of physical parameters to identify feature combinations that make the new deep learning approach achieve better accuracies, precisions, and recalls in leak detection.

The organization of the remaining sections of this paper is as follows. Section 2 reviews previous studies related to canal leakage detection based on satellite imagery data. Section 3 describes the technical details of the Convolutional Neural Network (CNN)-based leakage detection algorithm augmented by the inspection knowledge. Section 4 presents the experiment design for validation. Section 5 presents testing results to show the performance of the developed algorithm regarding accuracy, precision, and recall using images collected from diverse environments. This presentation of testing results includes a comparison of the performance of the developed PGNN approach against the performance of the conventional deep learning algorithm that uses raw images for training and water leak detection. Section 6 concludes the study and discusses the limitations of the developed algorithm and future research.

2. Literature review

This section synthesizes studies relevant to the use of remote sensing and machine learning techniques for water leak detection in multiple domains. Specifically, Section 2.1 reviews studies on canal leakage detection methods. Section 2.2 outlines the use of Physics-guided Neural Networks (PGNN) in various applications to show the potential of the physics-guided machine-learning approach for improving the image-based leak detections.

2.1. Canal leakage detection

An ideal solution to detecting water leaks across a canal system should be comprehensive, efficient, precise, and economical. Previous studies explored the use of sonar imagery and remotely operated vehicles or autonomous underwater vehicles in supporting underwater inspections [12]. However, these approaches require professional surveyors to collect data on-site. The efficiency and costs for the data collection become the bottlenecks that limit the wide adoption of these approaches in large canal networks that contain hundreds of miles of canals. Previous researchers have identified that remote sensing has the potential for efficient and effective water leakage detection [5,8,7]. The uses of remote sensing techniques for water leakage detection are time-and cost-effective compared with traditional, intrusive methods such as acoustic sensors [16]. Previous studies have proven that vegetation on the levee, the temperature in the surroundings, soil humidity are common indicators of canal leakages [20].

Huang et al. developed an airborne system mounted with red, near-infrared, and thermal sensors to collect multispectral images [8,7]. Combined with field reconnaissance, the researchers manually rate sections of canals in terms of wetness, grass growth, cracks on the levee. This method could identify leaking parts, but it is subjective. When inspectors are not familiar with particular environments and canal sections, the manual assessments are unreliable.

Zanganeh et al. used Landsat 8 satellite image processing techniques to locate leakages [28]. They showed that remote sensing techniques using free medium resolution satellite images could achieve early detection of leakages. The developed algorithm used a normalized difference vegetation indices (NDVI) to analyze the distribution of vegetation along the canals. The algorithm then used the K-means classification technique on the NDVI map to identify leakages. However, this method only considered the NDVI, while NDVI could hardly provide sufficient information for leakage detection in environments that mix buildings, plants, and other land covers. Besides, the K-means method needs the users to input a K value, but that K value estimated by the users could be inaccurate and misleading the clustering results. Although sensitivity analysis can help to find the optimal K values, the optimal K values could vary with different data sets.

The methods mentioned above are either subjective or requiring prior knowledge crafted by domain experts. Personal factors pose challenges to objective and consistent condition assessment of canal network spanning over in various geospatial environments – even the most experienced experts could not be familiar with all sections of canals in all possible contexts. Moreover, these methods focused on one or two environmental features (vegetation, temperature, soil humidity), while pointing out that none of those features alone could support robust, consistent, and reliable leak detection in various environments [8,28].

2.2. PGNN

Previous researchers have adopted computer vision, and machine learning approaches for civil infrastructure inspection tasks, such as pavement defect detection [14,19]. However, those approaches cannot work well in canal crack detection because the cracks of canal systems are usually under the water and invisible. Moreover, the conventional "black-box" neural network has one limitation - the trained model is solely dependent on the training data. In many cases, the predictions of the model could be inconsistent with the known laws of physics. Recent research proposed two categories of PGNN. The first category of PGNN uses physics theories to calculate and feeds features into neural networks. For example, Karpatne et al. proposed PGNN and applied the methodology in lake temperature modeling [13]. That study integrated the physical relationships between the temperature, density, and depth of water into the PGNN.

The second category of PGNN adopts physics-based loss functions by adding a physical-inconsistency term. For example, Yu et al. adopted a PGNN approach for aircraft dynamics simulation [27]. The researchers used the underlying physics of the aircraft dynamical system to construct a deep residual recurrent neural network. The results showed that PGNN has a better generalization potential and could produce physically meaningful results to improve the interpretability of the neural networks [13,27].

3. Methodology

The methodology developed by the authors consists of three parts (Fig. 1). Firstly, the authors developed a new method to utilize satellite images to evaluate the condition of canals by including more environmental features: land surface temperature (LST), Fractional vegetation cover (FVC), and soil moisture (TVDI). Existing studies mainly rely on Normalized Difference Vegetation Index (NDVI) for indicating the existence of vegetation that could reflect potential canal leakages [28]. The authors integrated LST and TVDI in addition to the vegetation-related index for canal leakage detection in complex urban environments. Secondly, the authors developed a PGNN to classify the canal sections as leaking sections and no-leaking sections based on historical canal maintenance records. The third step is the post-processing of the classification results of CNN. The classification algorithm predicts the leakages by separating the large satellite images into small windows. This step needs to geo-reference the small windows to locate these windows on the satellite images and help determine the leaking sections within those windows. More detailed illustrations of each step are as follows.

3.1. Water-leak-relevant physical feature engineering for augmenting satellite images with domain knowledge

The features in the input data of deep learning are important for the prediction. The quality and quantity of the features will have significant impacts on the model's classification performance. Based on the domain knowledge of irrigation canal management, LST, FVC, and TVDI tended to be reliable indicators of canal leakages [1,18]. For instance, if vegetation appears in a dry area where the plant is uncommon, it indicates that seepage may exist.

Similarly, water loss arisen from canal leakage influences the soil humidity and land surface temperature of the surrounding areas [8]. Some researchers used radar to detect soil humidity and used thermal cameras to detect land surface temperature for canal leakage detection [17]. The authors used the Landsat 8 satellite images to derive LST, FVC, and TVDI as the input features of the developed PGNN algorithm.

LST is a crucial indicator of water leakage [6]. The researchers used an approach called the Radiative Transfer Equation (RTE) to calculate the LST from high-resolution remote sensing images [26]. RTE represents the propagation of electromagnetic radiation through the earth's space. The processes affecting that propagation include absorption, emission, and scattering. Yu and his colleagues proposed a simple version radiative transfer equation expressed as follows [26],

$$R_{i,T_i} = \tau_{i,\theta} \times (\varepsilon_i \times R_{i,G} + (1 - \varepsilon_i) \times PR_{i,\downarrow}) + PR_{i,\uparrow} \tag{1}$$

where R_{i,T_i} refers to the sensor radiance of channel i based on the brightness temperature T_i. $R_{i,G}$ refers to the ground radiance. $PR_{i,\downarrow}$ and $PR_{i,\uparrow}$ refers to the downwelling and upwelling path radiance, respectively. $\tau_{i,\theta}$ refers to the atmospheric transmittance of channel i within the zenith angle θ. ε_i refers to the surface emissivity of channel i.

Moreover, $R_{i,G}$ is expressed by the law of Plank,

$$R_{i,G} = 2 \times ac^2/\left(\mu_i^5 \times \left(e^{ac/\mu_i bT_s} - 1\right)\right) \tag{2}$$

where a, b and c refer to the light speed, Planck constant, and the Boltzmann constant, respectively. μ_i is the wavelength of channel i.

$$T_s = \frac{C_1}{\mu_i ln(\frac{C_2}{\mu_i^5 (R_{i,T_i} - PR_{i,\uparrow} - \tau_i(1-\varepsilon_i)PR_{i,\downarrow})/\tau_i\varepsilon_i} + 1)} \tag{3}$$

where $C_1 = 14387.7\mu m \bullet K$, $C_2 = 1.19104 \times 10^8 W \bullet \mu m^4 \bullet m^{-2} \bullet sr^{-1}$.

T_s is the land surface temperature. The authors could estimate $PR_{i,\uparrow}$, $PR_{i,\downarrow}$ and τ_i from the radiative transfer model with the thermal radiance measured at the sensor level and the atmospheric parameters obtained with the radio sounding. Following Equation (3), the authors can derive LST.

Then, the researchers used the Temperature Vegetation Dryness Index (TVDI) for soil humidity estimation. TVDI is a parameter to normalize the surface soil moisture. The TVDI method combines visible, infrared, and thermal bands. Based on the previous research, TVDI is expressed as follows [25].

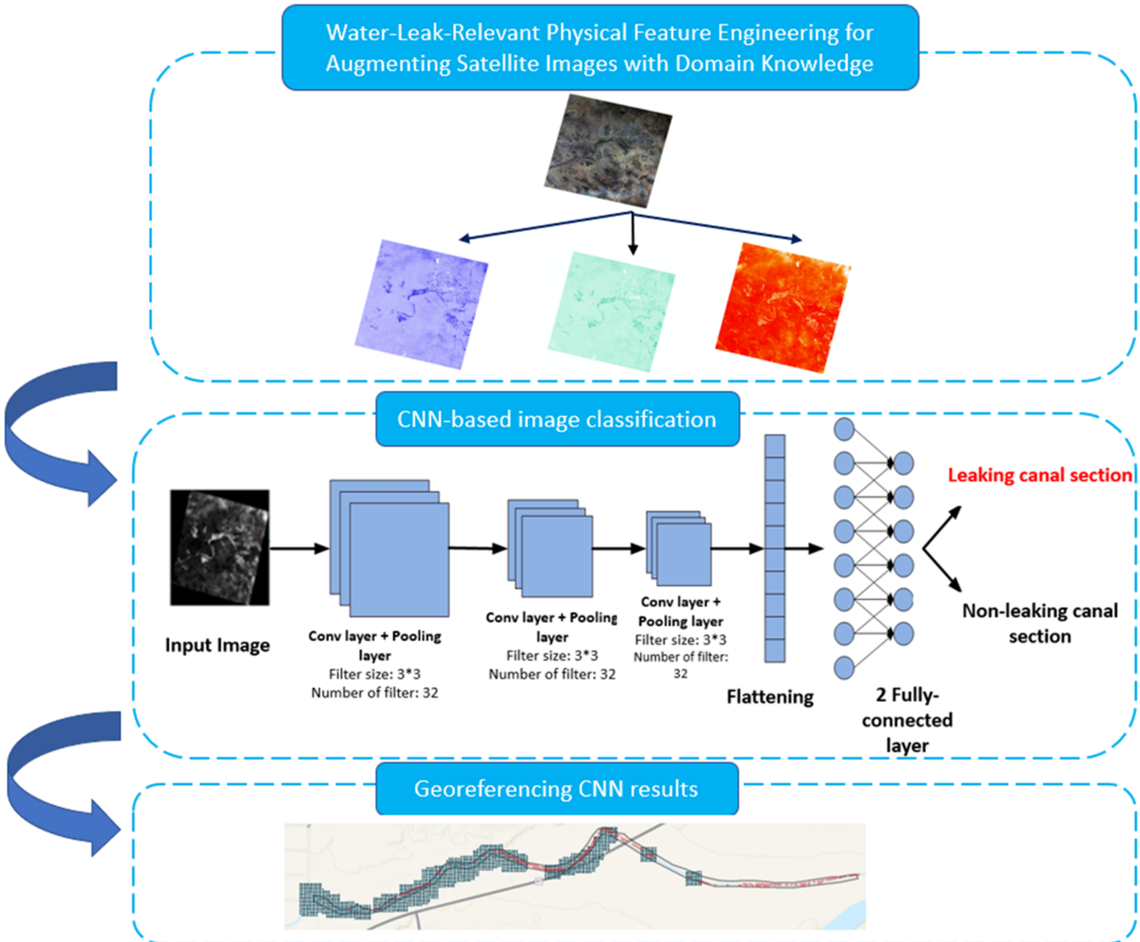

Fig. 1. An architecture for classification of canal conditions using satellite images.

$$TVDI = (T_{st} - T_{min-st})/(T_{max-st} - T_{min-st}) \tag{4}$$

where T_{st} refers to the surface temperature from Landsat 8. T_{min-st} and T_{max-st} denotes the minimum surface temperature and maximum surface temperature, respectively. T_{max-st} and T_{min-st} are calculated based on the following equations,

$$\begin{cases} T_{min-st} = a_1 + b_1 \times NDVI \\ T_{max-st} = a_2 + b_2 \times NDVI \end{cases} \tag{5}$$

where a_1 and b_1 are the coefficients used for controlling T_{min-st}, and a_2 and b_2 are the coefficients used for controlling T_{max-st}. $NDVI$ is expressed as follows,

$$NDVI = (w_{if} - w_r)/(w_{if} + w_r) \tag{6}$$

where w_{if} and w_r refer to the near-infrared and red wavebands, respectively.

FVC is the ratio between the vertically projected area of vegetation and the total surface extent [23]. FVC is widely used to describe vegetation quality. The authors implemented the linear mixture model, which has been widely applied for the estimation of FVC to generate the vegetation coverage [4].

$$FVC = \frac{NDVI - NDVI_s}{NDVI_v - NDVI_s} \tag{7}$$

where $NDVI_s$ *is the minimum of* NDVI in the studied area and $\mathrm{NDVI_v}$ is the maximum of NDVI in the studied area [4].

3.2. CNN-based image classification

The water leakage detection based on satellite image analysis is an image-based classification problem of regions captured in satellite images. In other words, the algorithm developed by the researchers take satellite images as inputs and classify the areas of the photos as leaking or non-leaking sections. Machine learning methods can solve such a classification problem by training a classification model based on sample images and applying the model to new images for the image region classification.

Rather than sending surveyors to the canals and conduct inspections, the machine learning algorithm can take large amounts of image samples and learn from the examples to estimate a set of parameters for a neural network model. The resulted neural network can classify new images based on the training samples. This parameter estimation process of the neural network model is the "training" process. The trained neural network model uses the similarity between training samples and images for classification. Deep learning is a new generation of the machine learning algorithm. Deep learning is modeled after the human brain, which consists of many layers of neurons allowing it to make complex decisions. In this research, the researchers used historical maintenance data to train a deep learning model. The deep learning algorithm can achieve more reliable classifications given large amounts of historical image samples [29].

The research team extracted feature images of the LST, FVC, and TVDI from satellite images. With these three feature images, the research team reconstructed a three-channel image as the input of the convolutional neural network. Using a sliding window technique, the researchers segmented the satellite image into 8*8 windows with a 1-

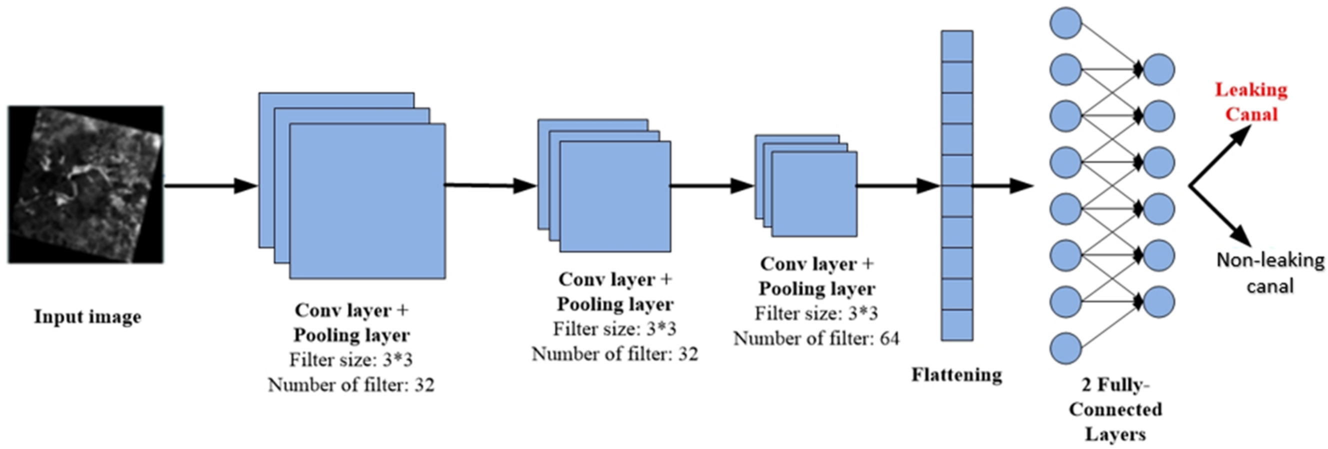

Fig. 2. Convolutional Neural Network architecture.

pixel step of moving the window on satellite images. Fig. 2 shows the architecture of the model. This model includes three convolutional layers and two fully connected layers. In this model, the research team conducted a binary classification to categorize image windows. The output is the condition of each small window being leaking or no-leaking (e.g., canal section has no leakages, or the canal section has leakages).

The architecture of the proposed CNN consists of the conv-pooling layer, the fully-connected layer, and the classification layer. The input image has dimensionality 8*8*3, and the three channels are LST, FVC, and TVDI, which are generated from a satellite image. The researchers resized the image to 128*128*3 to feed into the CNN. The conv-pooling layer includes three sub-layers; the first and second conv-pooling layers use 32 filters within the 3*3 window. The last conv-pooling layer uses 64 filters within the 3*3 window. Then a two-layer fully connected layer processes the output of flattening the result generated by the last conv-pooling layer. Finally, the classification layer uses a "softmax" function to perform a binary classification to determine whether each image belongs to no-leaking or leaking condition. "Softmax" is a function that can output a vector, which represents the probability distribution over the predicted output classes [15]. The predicted class is the class with the highest probability output from the softmax function.

After collecting the satellite image and locations of repairs, the next step was to segment the satellite image into multiple 8*8 windows and annotate the windows. The annotation procedure is different from traditional computer vision annotation that visually labeled every image based on subjective understanding. In this project, the locations of repairs are labeled on the Google Earth satellite image first, followed by overlaying the repair locations on the Landsat 8 images. This overplayed product helps the research team identify the pixels which crossed the physically repaired sections of canals automatically rather than labeling each image. If the 6*6 square (red square in Fig. 3) in the 8*8 window contains a repair location, then the research team labeled the window as a window containing leaking sections (called "leaking window" hereafter), and vice versa. Such labeling is more objective and reflecting the actual repairing needs for leaking parts.

3.3. Geo-referencing the results generated by the CNN algorithm

The traditional CNN algorithm gives the prediction result of each image sent to the algorithm. CNN predicts the conditions of every window being "no-leaking" or "leaking." However, different from the other imagery data, the windows generated from satellite images are geo-referenced [29]. The research team projected each window back to the map to locate which sections of canals are having leaking parts. For this purpose, the research team used ArcGIS Desktop to geo-reference the windows.

3.4. Performance metrics for evaluating the developed PGNN approach

This section presents the performance evaluation approach used to quantify the performance of the developed PGNN classification algorithm. The authors also use the same performance metrics to compare the performance of the developed PGNN algorithm and a conventional deep learning approach that uses raw satellite images for training and testing the machine learning model. Such conventional deep learning methods use all 11 channels in the raw image pixels for leak classification. PGNN approach, on the other hand, uses the three physical features as three channels to replace the 11 channels of the raw imagery data in machine learning model training and testing. Fewer channels would make the training process of the deep learning models much more computationally efficient while having risks of losing some information in the raw data that has 11 channels. The authors use the performance metrics below to compare the performance of PGNN and conventional deep learning model trained on raw satellite images in leak detections to answer this question: *could PGNN save the training time of the machine learning model without losing too much leak detection performance compared with the conventional deep learning?*

The performance evaluation generates four values, including true positive (TP), false positive (FP), false negative (FN), and true negative (TN). For example, "true positive" means that the PGNN algorithm predicted the canal section had cracks, and the section has cracks in reality. In this case, if the SRP team repairs the section predicted by the PGNN algorithm, they would be able to allocate the resources correctly.

Using Equation (8), the authors use accuracy, precision, and recall for quantitatively assessing the classification performance of the developed algorithm.

$$Precision = \frac{TP}{TP + FP} Recall = \frac{TP}{TP + FN} Accuracy = \frac{TP + TN}{TP + TN + FP + FN} \tag{8}$$

Equation (8) Precision, recall, and accuracy of the algorithm.

4. Experiments

The researchers used the past maintenance records of the canal sections to predict the water leakage of other canal sections that will be maintained in the future. This section describes the studied areas the researchers chose for the experiments and the data preparation process for the tests.

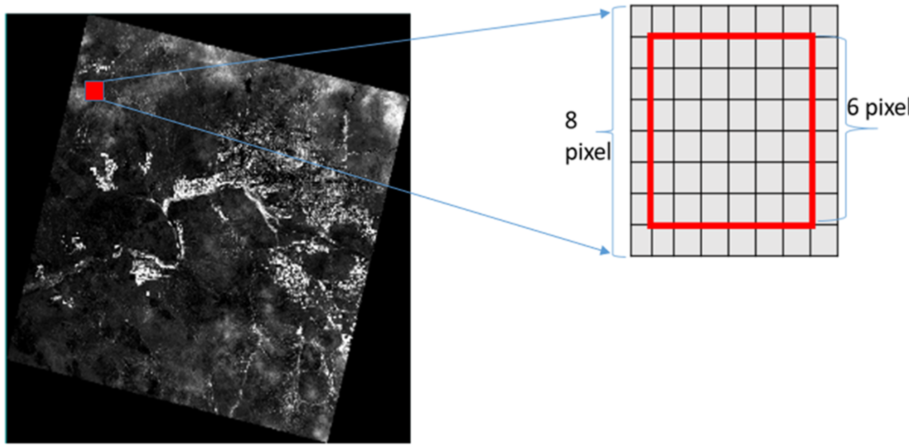

Fig. 3. Annotation of 8*8 windows extracted from satellite imagery data.

4.1. Studied areas

Arizona Canal, South Canal, and Western Canal are three main canals belonging to the SRP canal system. Arizona Canal and South Canal crossed rural areas, while the Western Canal crossed urban areas. The authors chose these areas to compare the performance of the algorithm in different environments. Fig. 4 shows the rural and urban study areas.

4.2. Data preparation

The researchers chose Landsat 8 satellite images, which are free to the public since 2013. The Landsat 8 satellite can take images of the entire earth every 16 days [28]. Landsat 8 has 11 bands, multispectral bands 1–7 and 9 (30-meter pixel size), panchromatic band 8 (15-meter pixel size), and thermal infrared bands 10–11. Based on the algorithms developed in previous studies, the research team extracted environmental features, including LST, FVC, and TVDI [25,26,30].

After the dry up and repair of the South Canal, the research team used the repair information provided by SRP to locate the concrete cracks for repairing (Fig. 5) and labeled the locations of leakage based on the maintenance records using ArcGIS (Fig. 6). ArcGIS can import satellite images and let users select the region of interest. The authors used ArcGIS to mark the regions where the repairing happened. The sliding-window techniques then segment the satellite images into the 8*8 window (64 pixels each window) with a step at 1 pixel. The authors filtered out the windows that do not cross the canal and then labeled the windows that cross the canal as leaking and non-leaking. Finally, the authors collected a dataset of 6360 windows with 4409 windows as leaking and 1951 windows as non-leaking (Table 1).

The authors made different transformations, including flip and rotation, to the original images to increase the training dataset. Such augmentation of the training data set has the name "Data augmentation" in the literature [22]." The augmented dataset has 10,000 windows. Finally, the researchers used the expanded dataset to train and

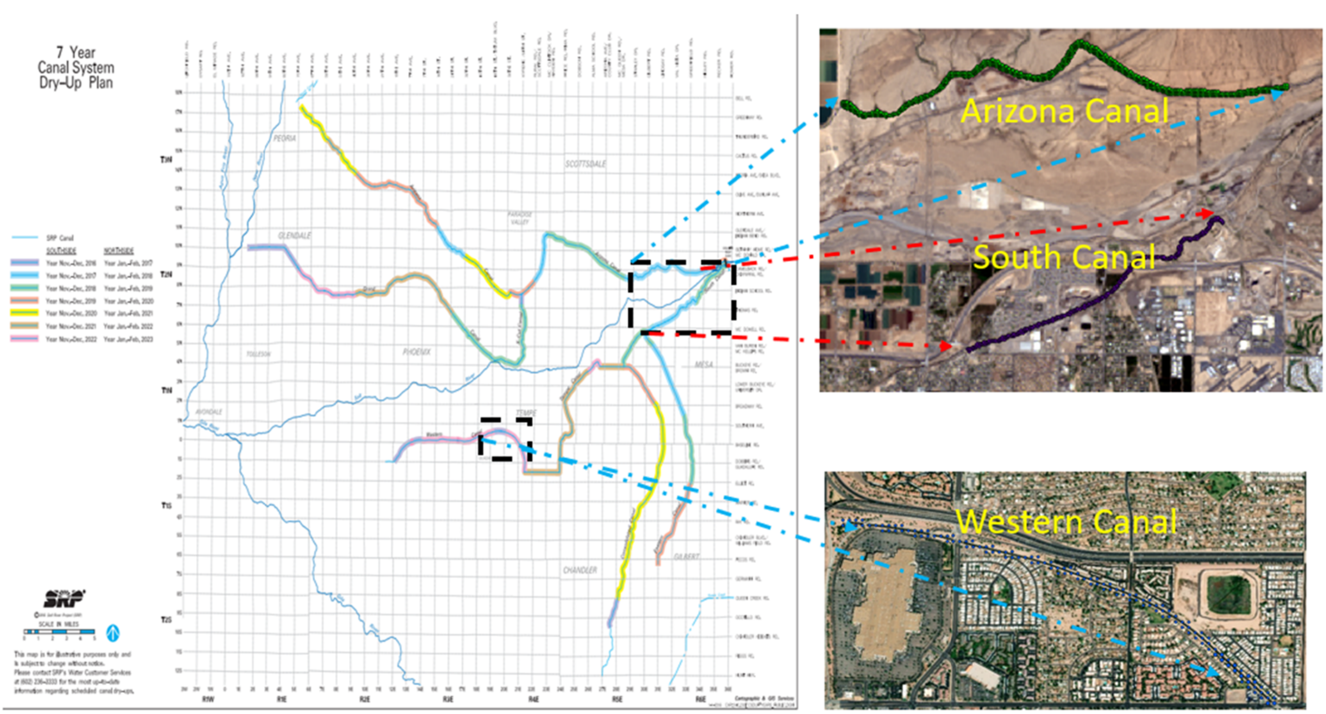

Fig. 4. Study Areas: Arizona Canal and South Canal are in rural areas, while Western Canal is in urban areas.

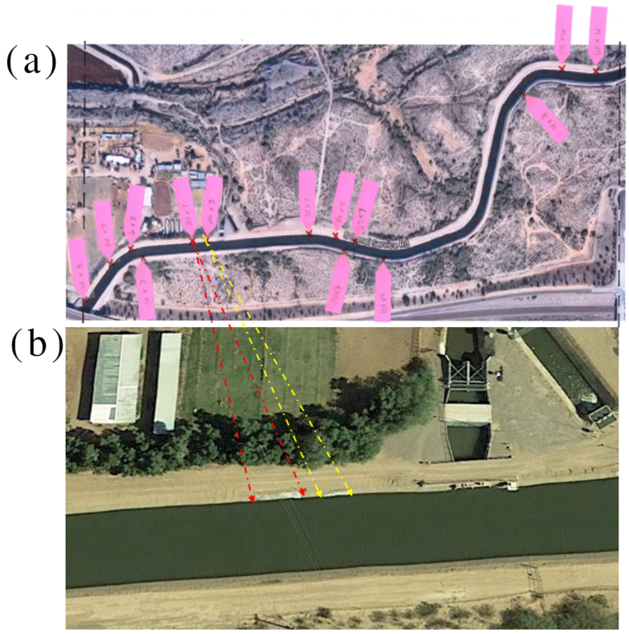

Fig. 5. (a) An example of the maintenance records that highlight the dimensions and locations of leaking parts of the canal. (b) The actual location of leakage marked by surveyors on canal riverbed, image from Google Earth.

test the proposed method with 8000 windows for training, and 2000 windows for testing. The authors also tested the performance of the developed algorithm in different geospatial environments. As shown in Fig. 7, canals sections used for testing the developed algorithm include canal sections in both rural and urban environments. The canal sections crossing urban areas have a complex geospatial environment with various land covers. The canal sections crossing rural areas have a relatively simple geospatial environment where most of the areas are farming or empty desert lands.

5. Results

This section presented the results of the experiments and some discussions about the findings. The researchers extracted the LST, TVDI, and FVC from satellite images (Section 5.1) and detected water leakages using the proposed methodology (Section 5.2). Then, the researchers tested the performance of the algorithm on different landcovers (i.e., urban and rural areas) to evaluate the performance of the algorithm (Section 5.3). Finally, the authors compared the developed PGNN and the conventional deep learning approach to clarify the performance and computational efficiency-related advantages of the PGNN approach (Section 5.4).

5.1. Environmental feature extraction results from satellite images

Following the feature extraction methods described in Section 3.1, the researchers extracted the LST, FVC, and TVDI from satellite images.

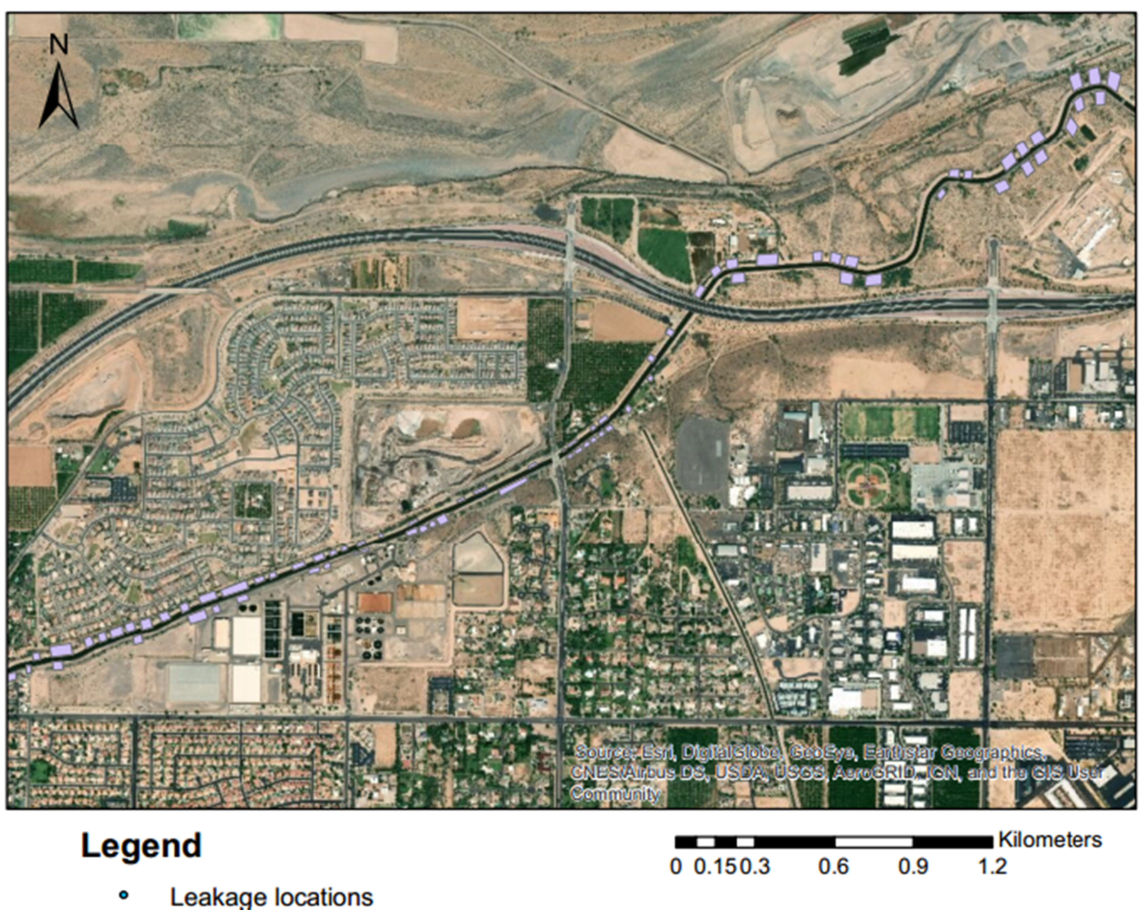

Fig. 6. Mapping the leakage locations using the ArcGIS platform: the purple boxes of different sizes indicate the dimensions and areas of the leakages.

Table 1
Data description.

Canal	Area type	Satellite image date	Number of leaking windows	Number of non-leaking windows
Western Canal	Urban	11/01/2016	179	698
South Canal	Rural	10/19/2017	1684	271
Arizona Canal	Rural	01/23/2018	2546	982

Fig. 7. Pictures showing the difference between rural and urban areas of canal sections.

The Landsat 8 image has a resolution of 30 m, which means every pixel in the image represents 30 m. Figs. 8–10 shows the results of deriving LST, FVC, and TVDI using Landsat 8. The higher value of the pixel in the plant cover image represents more vegetation in that area. Similarly, the more significant value of the pixel in the land surface temperature result represents a higher temperature in that area. However, the smaller value of the pixel in soil humidity image represents more soil.

5.2. Leakage detection results using CNN

The researchers evaluate the performance of the proposed algorithm in terms of accuracy, precision, and recall (Equation (8)). The researchers used the collected dataset (Section 4.2) that includes canals in different landcover from the year 2016 to the year 2019. The researchers used all three environmental features LST, FVC, and TVDI, to

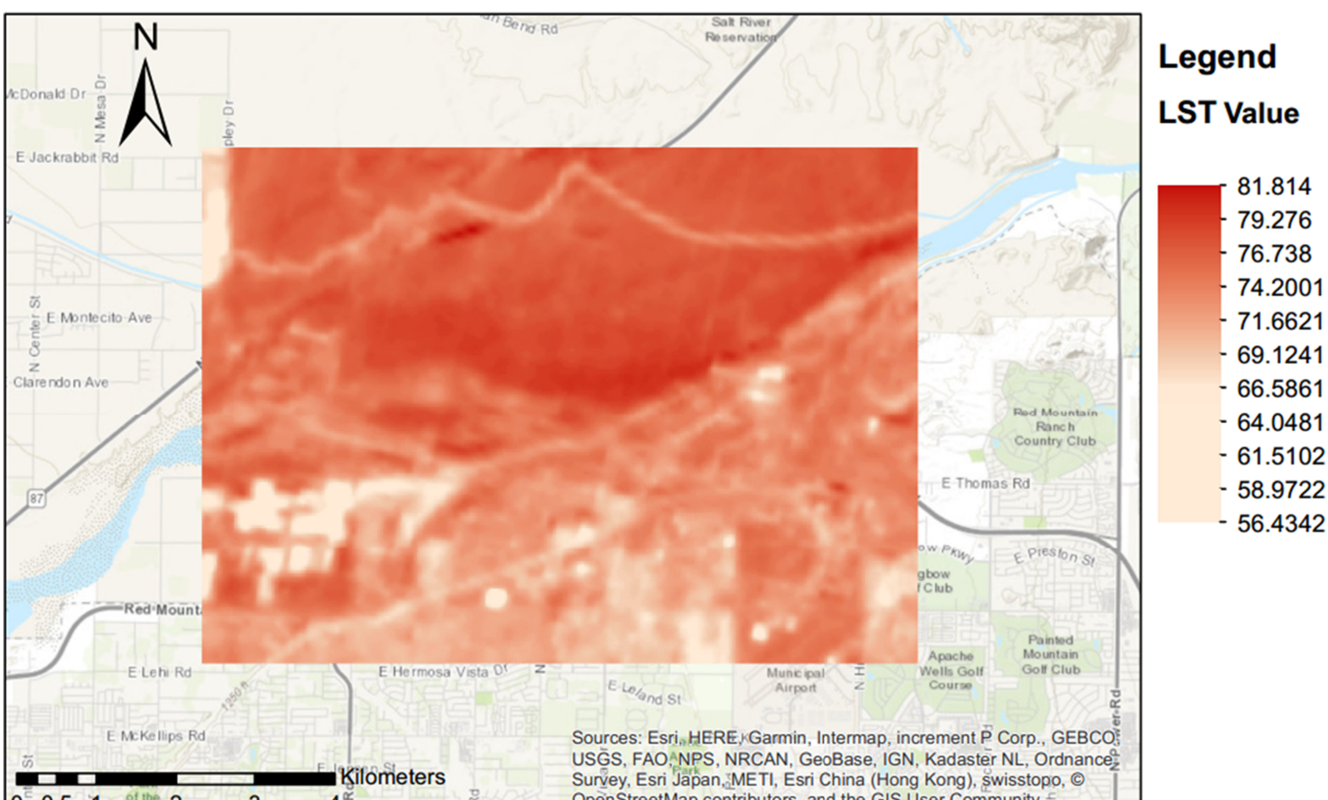

Fig. 8. LST result in the studied area.

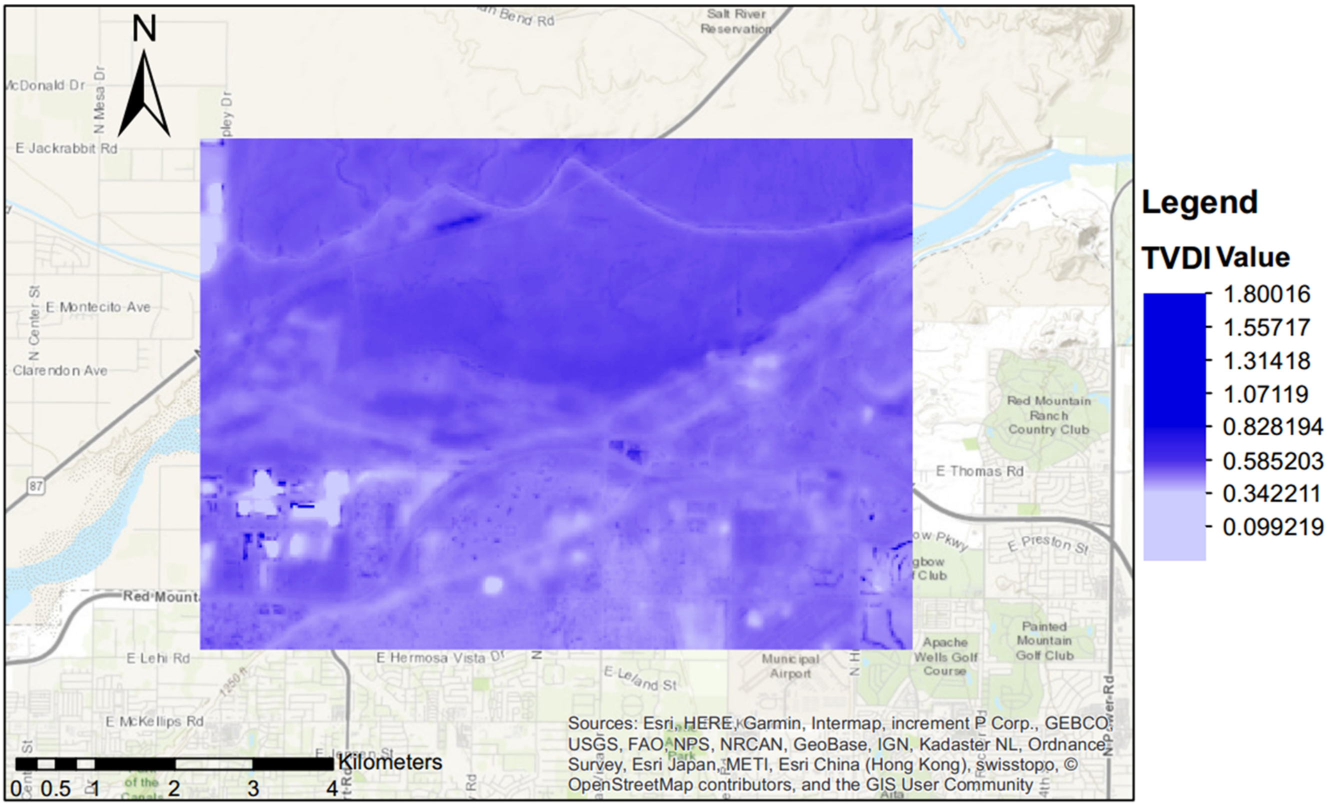

Fig. 9. TVDI result in the studied area.

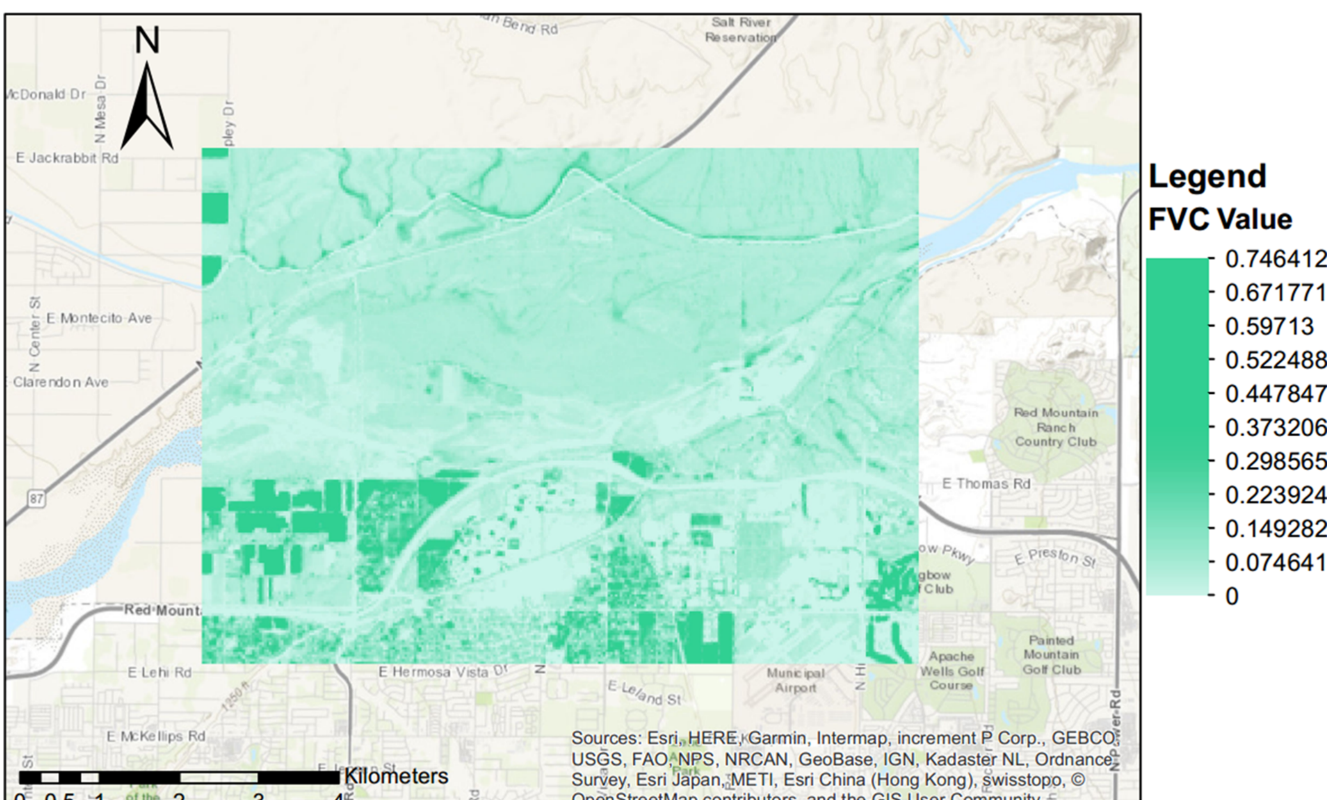

Fig. 10. FVC result in the studied area.

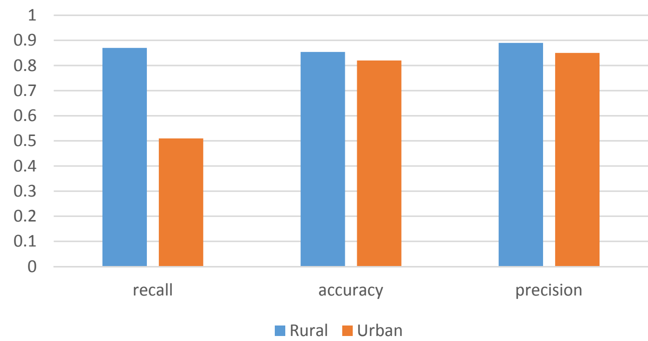

Fig. 11. Comparison of the performance in different environments.

train the CNN model. The precision of the methodology is 86%, the recall is 86%, and the accuracy is 85%.

Moreover, the researchers tested the performance of the trained model in different environments of different land covers. Fig. 11 showed the recall, accuracy, and precision of the same trained model tested in urban and rural areas. The researchers found that the trained model has a more reliable performance in rural areas. This finding coincides with the fact that urban areas have more complex geospatial environments that make urban areas more difficult than rural areas to detect canal leakages.

5.3. Test on environmental feature combination

One major limitation of the neural network is that the neural network is similar to the "black box." The trained model can establish a relationship between input and output, using millions of parameters. However, the neural network cannot tell what happened inside the "black box" and which parts of the input are more informative to the output. Knowing which features are more influential to canal leakage detection is important to engineers. The research team proposed to use different combinations of environmental features as training data and test the performance of the proposed algorithm in both rural and urban areas. Because there are three environmental features, the research team tested seven feature combinations listed in Table 2. The tests of environmental features used different inputs to train and test the neural network. All seven experiments use the same architecture of the deep learning neural network.

Table 3 shows the results of different feature combinations in different various geospatial environments. The researchers evaluated the performance of different feature combinations in terms of accuracy, precision, and recall. Overall, the feature combinations of (LST, FVC, TVDI) and (LST, FVC) have the best performance in both rural and urban areas (Fig. 12).

From the test results in Table 3, the research team conducted a comprehensive analysis and came to the following findings:

1) As Fig. 12 shows, using a combination of multiple features as input outperforms using a single feature as the input. Overall, the feature combinations of (LST, FVC, TVDI), and (LST, FVC) have the best performance.

Table 2
Feature input for different environmental feature combinations.

Experiment number	1	2	3	4	5	6	7
Input	LST, FVC, and TVDI	LST and FVC	LST and TVDI	FVC and TVDI	LST	FVC	TVDI

Table 3
Performance of different feature combinations at various geospatial environments.

Features	Testing area	recall	accuracy	precision
LST, FVC, TVDI	Rural	0.87	0.854	0.89
	Urban	0.51	0.872	0.94
	Rural and Urban	0.86	0.857	0.86
LST	Rural	0.80	0.79	0.79
	Urban	0.56	0.86	0.66
	Rural and Urban	0.81	0.81	0.81
FVC	Rural	0.79	0.79	0.78
	Urban	0.50	0.5	0.43
	Rural and Urban	0.80	0.81	0.81
TVDI	Rural	0.50	0.42	0.21
	Urban	0.5	0.5	0.43
	Rural and Urban	0.5	0.5	0.25
LST, FVC	Rural	0.78	0.77	0.78
	Urban	0.86	0.85	0.85
	Rural and Urban	0.79	0.79	0.79
LST, TVDI	Rural	0.58	0.52	0.58
	Urban	0.5	0.23	0.33
	Rural and Urban	0.5	'0.52	0.5
FVC, TVDI	Rural	0.58	0.52	0.34
	Urban	0.5	0.27	0.58
	Rural and Urban	0.5	0.36	0.5

2) All the feature combinations, except for using TVDI, have a more reliable performance in rural areas than urban areas. The feature combination of TVDI has unreliable performance in both rural and urban areas. The performance of TVDI in rural areas is worse than the performance of TVDI in urban areas (Fig. 12).
3) For Fig. 13, the importance of a single feature has a sequence as LST > FVC > TVDI from strong to weak. LST is the most reliable environmental feature to detect canal leakage while TVDI has the worst performance.
4) The research team also analyzed how adding environmental features may influence the performance of existing feature combinations. From Figs. 14–16, the research team compared how added environmental features can affect the current feature combination. The results showed that adding LST and FVC can improve the performance of the existing feature combination. Whereas, adding TVDI tends to damage the performance of the algorithm. The potential reason for this phenomenon is that the algorithm using Landsat 8, a medium resolution satellite image, to estimate soil humidity is not reliable.

5.4. Comparison between the developed PGNN approach versus a conventional deep learning algorithm trained on raw satellite images

The authors developed the PGNN approach to increase the interpretation of the neural network. The expectation is that PGNN could help engineers explain and understand how environmental conditions could indicate the canal leaking conditions. To fully explore the value of the PGNN approach, the authors compared the developed PGNN approach against the conventional deep learning algorithms trained on raw satellite images. The authors used the same augmented dataset with 8000 images as training and 2000 images as testing. The only difference is that for the conventional deep learning approach, the authors used raw satellite images for training and testing the machine learning model.

For the PGNN approach, the authors used all three features, including LST, FVC, and TVDI. The authors used a desktop computer composed of an Intel CPU and an NVidia 1080Ti graphics card. As for training time, the PGNN approach took 2 h to train 10,000 iterations. The conventional deep learning approach took approximately 5 h to train.

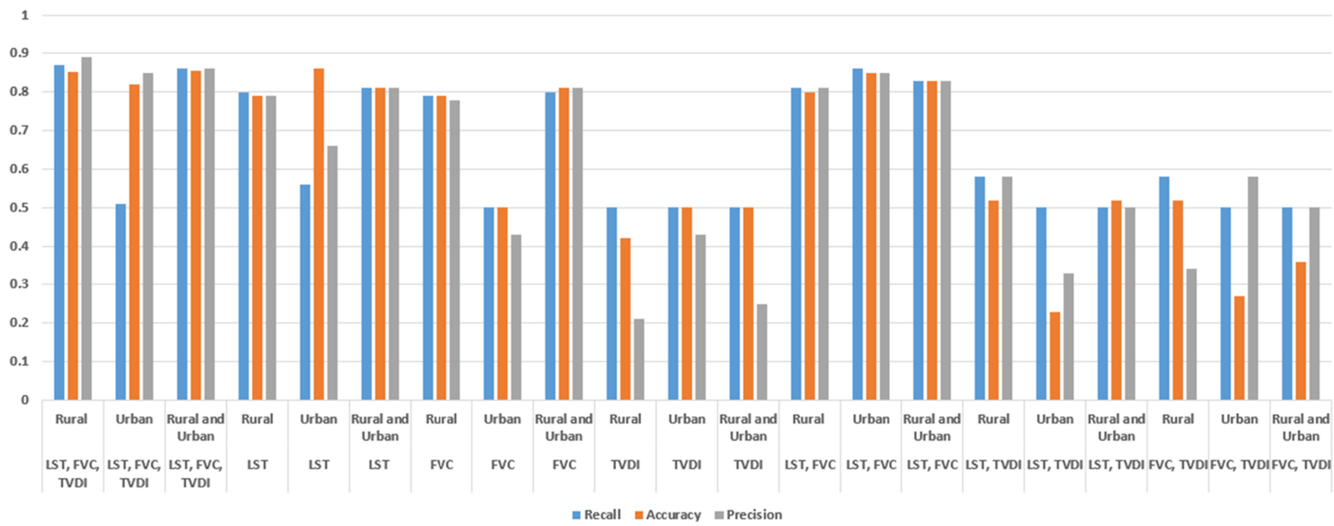

Fig. 12. Performance of seven feature combinations on different landcover.

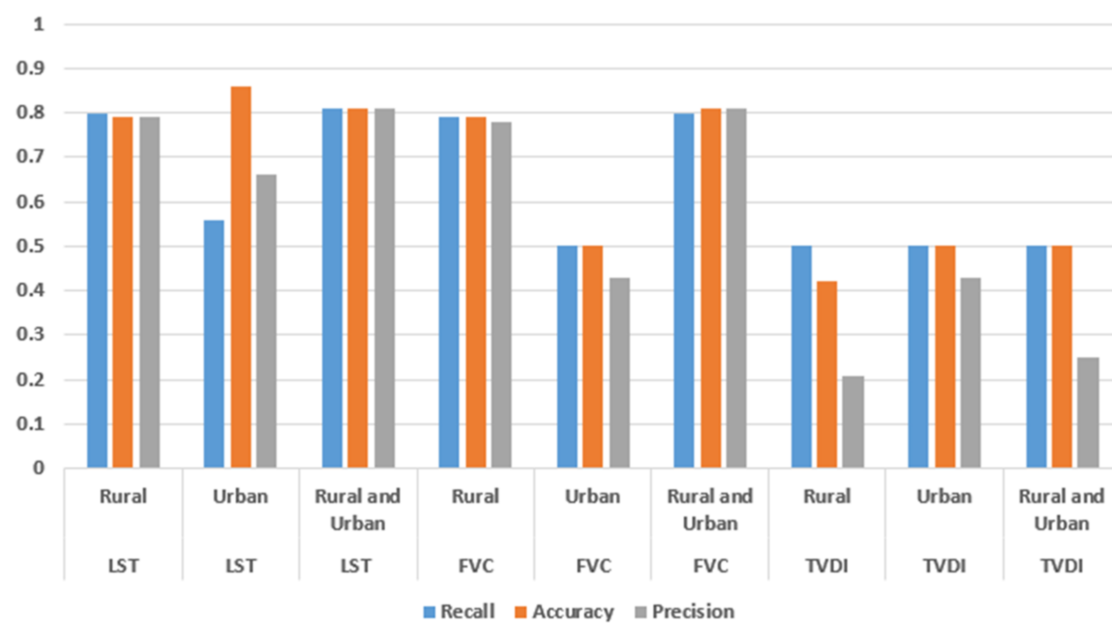

Fig. 13. Performance of single environmental feature on different landcover.

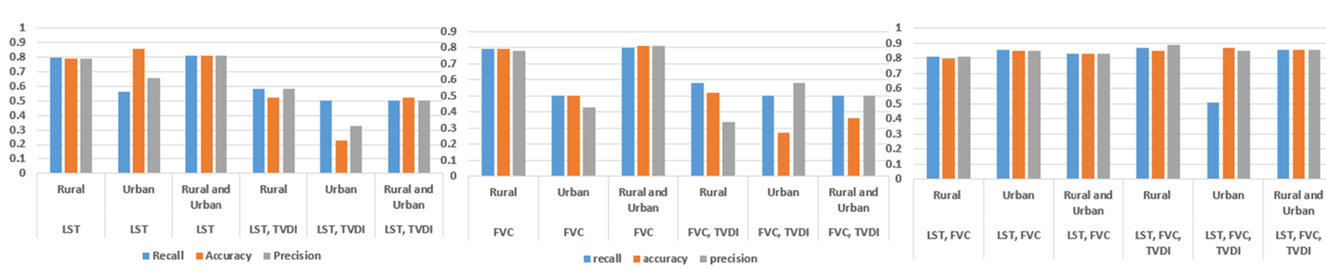

Fig. 14. Performance of the proposed algorithm after adding TVDI to existing feature combinations.

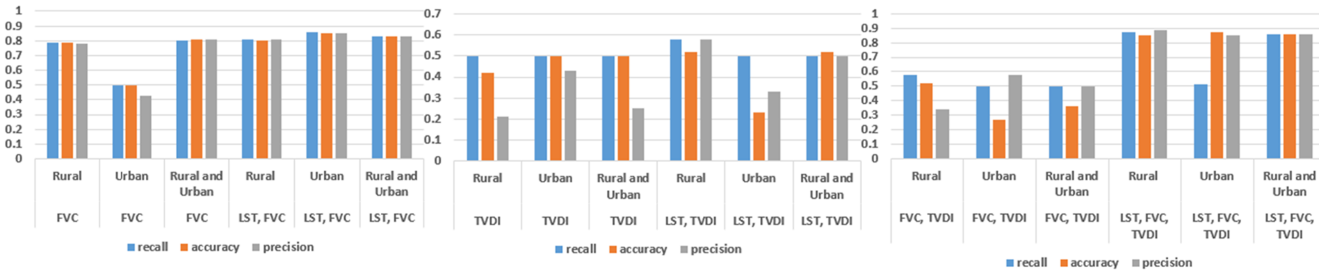

Fig. 15. Performance of the proposed algorithm after adding LST to existing feature combinations.

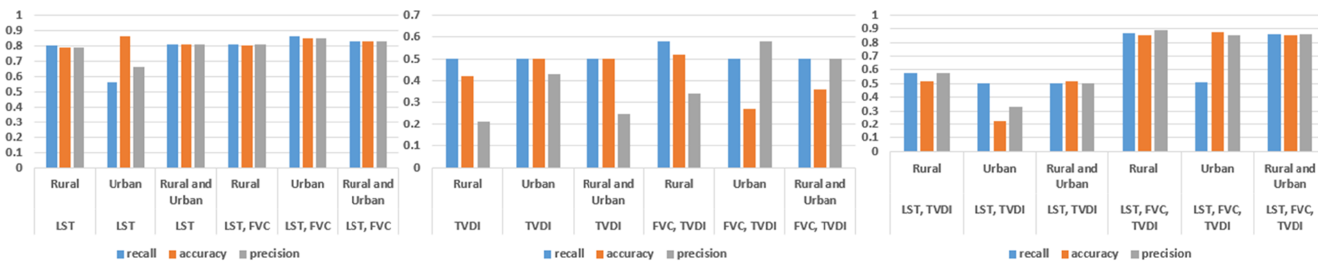

Fig. 16. Performance of the proposed algorithm after adding FVC to existing feature combinations.

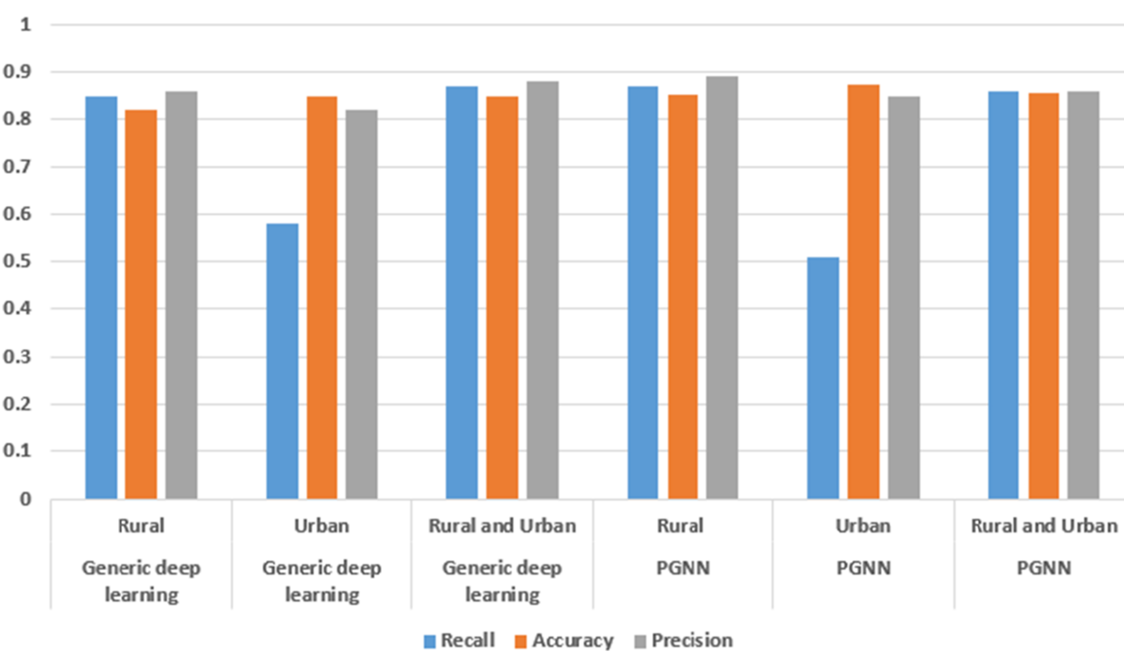

Fig. 17. Comparison between conventional deep learning and the developed PGNN approach.

As shown in Fig. 17, conventional deep learning can achieve similar accuracy, precision, and recall as the PGNN approach, although training the conventional deep learning model takes more time. Another major advantage of the PGNN approach is that the channels of input have physical meaning, which can help engineers understand which features are more useful for detecting canal leakages.

6. Discussions

6.1. Contributions and implications

The results indicate that a medium resolution satellite image can achieve excellent performance in canal leakage detection. A PGNN can achieve reliable classification accuracy, precision, and recall while being more computation efficient than conventional deep learning. Furthermore, the researchers found that the proposed algorithm has a better performance in rural areas than urban areas because the geospatial contexts in urban areas are more complicated than that of rural areas. To increase the interpretability of the neural network, the researchers integrated remote sensing knowledge to derive environmental features and tested how different combinations can influence the performance of the proposed algorithm. The researchers found that LST tends to be the most important environmental feature among LST, FVC, and TVDI. Also, the researchers found that combinations of LST, FVC, and LST, FVC, and TVDI have the best performance in different landcover. These findings can provide an in-depth understanding of the interactions between environmental conditions and civil infrastructures. Moreover, these findings will lead to new knowledge about how environmental conditions influence civil infrastructure maintenance.

Moreover, the data library established and processed in this research, as well as the neural network model, will help engineers develop a decision-making process that relies on timely and high-quality field data and predictions based on such data. These automated remote sensory data processing techniques can help engineers to fully utilize large amounts of data available to them through multiple sources and expose them to large amounts of free remote sensory data sources, such as Landsat 8, Planet, and other satellite images potentially useful for civil infrastructure maintenance. These automated data processing algorithms can significantly reduce the data processing time and workforce needs through automated algorithms.

6.2. Limitations and recommendations for future research

First, the limitation of this research is that the current algorithm can only classify canal sections into leaking and non-leaking categories because collecting and labeling the satellite images takes lots of effort and time. A more efficient method that can label the satellite image into multiple levels of leakage will make the proposed algorithm more reliable and useful. Second, the resolution of the prediction results of the proposed algorithm is in the window-level. Each window is 8 pixels * 8 pixels, which covers a 240 m * 240 m area. To detect canal leakage with higher accuracy, the researchers may need to explore the use of the high-resolution satellite image such as Planet.

As for future work, the research team will improve the current work with the following parts to create more scientific and economic values. The first part will be extending the algorithm for additional anomaly detection tasks. The current algorithm can only classify canals as leaking and non-leaking because the established dataset has only two categories of labels. However, this algorithm could classify canal sections into multiple levels of water leakage if provided a data library that labeled canal sections into multiple levels of water leakage. The second part will be transplanting this method to other civil facilities such as underground pipes. The researchers will focus on producing a predictive spatiotemporal model that takes environmental conditions and any other physical and technical parameters of civil infrastructure systems as “contextual conditions” to predict anomaly in civil infrastructures.

7. Conclusions

This research study explored the methodology of using multispectral satellite imagery to assist canal condition assessment. The research team used remote sensing algorithms to extract environmental features from multispectral satellite images. Then the research team adopted a PGNN that can automatically detect the leaking sections of canals on satellite images. To establish the dataset for the PGNN, the research team collected Landsat 8 satellite image and canal maintenance records from 2016 to 2019 in different areas.

Through the training and testing process, the proposed algorithm achieved the precision at 86%, recall at 86%, and accuracy at 85%. Furthermore, the research team tested different combinations of environmental features and explored how different combinations of environmental features influenced the performance of the developed algorithm in different geospatial environments. The feature combinations of (LST, FVC) and (LST, FVC, TVDI) are the two robust feature combinations that can detect canal leakages in diverse geospatial environments. This research study sheds light on detecting water leakage through the integration of remote sensing techniques and deep learning.

Declaration of Competing Interest

The authors declare that they have no known competing financial interests or personal relationships that could have appeared to influence the work reported in this paper.

Acknowledgments

This material is based on work supported by the Joint Research Program of Salt River Project (SRP). SRP’s support is gratefully acknowledged. Any opinions, findings, conclusions, or recommendations expressed in this paper are those of the authors and do not necessarily reflect the views of SRP.

References

[1] M. Arshad, R. Gomez, A. Falconer, W. Roper, M. Summers, A remote sensing technique detecting and identifying water activity sites along irrigation canals, Am. J. Environ. Eng. Sci. 1 (1) (2014) 19–35.
[2] S. Carter, Controlling Water Seepage in Canals with Canal Liners.
[3] J. Chen, P. Tang, T.E. Rakstad, Integrated analysis of aerial and terrestrial imagery data for efficient and effective water loss mapping of a canal system, in: Pipelines 2017: Condition Assessment, Surveying, and Geomatics - Proceedings of Sessions of the Pipelines 2017 Conference, 2017, p. 136–147.
[4] G. Gutman, A. Ignatov, The derivation of the green vegetation fraction from NOAA/AVHRR data for use in numerical weather prediction models, Int. J. Remote Sens., Taylor & Francis 19 (8) (1998) 1533–1543.
[5] D.G. Hadjimitsis, A. Agapiou, K. Themistocleous, D.D. Alexakis, G. Toulios, S. Perdikou, A. Sarris, L. Toulios, C. Clayton, Detection of water pipes and leakages in rural water supply networks using remote sensing techniques, Remote Sens. Environ. Integr. Approaches (2013).
[6] Y. Huang, E. Associate, G. Fipps, E.A. Engineer, Thermal imaging of canals for remote detection of leaks : evaluation in the united irrigation district thermal imaging of canals for remote detection of leaks: evaluation in the united irrigation district 1, Water Resour., (November) (2008).
[7] Y. Huang, G. Fipps, S.J. Maas, R.S. Fletcher, Airborne remote sensing for detection of irrigation canal leakage, Irrigat. Drain. 59 (2010) 524–534.
[8] Y. Huang, G. Fipps, S.J. Maas, R.S. Fletcher, Airborne remote sensing for detection of irrigation canal leakage, Irrig. Drain. 59 (5) (2010) 524–534.
[9] O. Hunaidi, W.T. Chu, Acoustical characteristics of leak signals in plastic water distribution pipes, Appl. Acoust., Elsevier 58 (3) (1999) 235–254.
[10] O. Hunaidi, P. Giamou, Ground-penetrating radar for detection of leaks in buried plastic water distribution pipes (1998).
[11] U.S.D. of the Interior, Canal Operation and Maintenance : Concrete Lining and Structures (2017).
[12] A. Inzartsev, A. Pavi, AUV application for inspection of underwater communications, Underwater Vehicles (December) (2009).
[13] A. Karpatne, W. Watkins, J. Read, V. Kumar, Physics-guided Neural Networks (PGNN): An Application in Lake Temperature Modeling, arXiv (2017).
[14] C. Koch, K. Georgieva, V. Kasireddy, B. Akinci, P. Fieguth, A review on computer vision based defect detection and condition assessment of concrete and asphalt civil infrastructure, Adv. Eng. Inf., Elsevier Ltd 29 (2) (2015) 196–210.
[15] A. Krizhevsky, I. Sutskever, G.E. Hinton, ImageNet classification with deep convolutional neural networks, Advances in Neural Information Processing Systems, (2012).
[16] C.A. Martin, T.K. Gates, Uncertainty of canal seepage losses estimated using flowing water balance with acoustic Doppler devices, J. Hydrol., Elsevier B.V. 517 (2014) 746–761.
[17] M.D. Nellis, Application of thermal infrared imagery to canal leakage detection, Remote Sens. Environ. (1982).
[18] C. Operation, Canal Operation and Maintenance : Concrete Lining and Structures, (November) (2017).
[19] S.C. Radopoulou, S.M. Asce, I. Brilakis, M. Asce, Automated Detection of Multiple Pavement Defects (2016).
[20] B. Saha, A critical study of water loss in canals and its reduction measures, Int. J. Eng. Res. Appl. 5 (3) (2015) 53–56.
[21] Salt River Project, 2015 SRP Annual Report, Annual Report, 2015.
[22] C. Shorten, T.M. Khoshgoftaar, A survey on image data augmentation for deep learning, J. Big Data, Springer International Publishing 6 (1) (2019).
[23] W. Song, X. Mu, G. Ruan, Z. Gao, L. Li, G. Yan, Estimating fractional vegetation cover and the vegetation index of bare soil and highly dense vegetation with a physically based method, Int. J. Appl. Earth Obs. Geoinf., Elsevier B.V. 58 (2017) 168–176.
[24] T. Tucciarelli, A. Criminisi, D. Termini, Leak analysis in pipeline systems by means of optimal valve regulation, J. Hydraul. Eng. (1999).
[25] S.M.Z. Younis, J. Iqbal, Estimation of soil moisture using multispectral and FTIR techniques, Egypt. J. Remote Sens. Space. Sci., Authority for Remote Sensing and Space Sciences 18 (2) (2015) 151–161.

[26] X. Yu, X. Guo, Z. Wu, X. Yu, X. Guo, Z. Wu, Land surface temperature retrieval from Landsat 8 TIRS—comparison between radiative transfer equation-based method, split window algorithm and single channel method, Remote Sens., Multidisciplinary Digital Publishing Institute 6 (10) (2014) 9829–9852.
[27] Y. Yu, H. Yao, Y. Liu, Aircraft dynamics simulation using a novel physics-based learning method, Aerosp. Sci. Technol. 87 (2019) 254–264.
[28] R. Zanganeh, B. Mojaradi, E. Jabari, Leak Detection from the Buried Water Transmission Pipeline Using Landsat 8 Satellite Images (Case Study of the Kosar Water Transmission Pipeline), International Conference on Civil Engineering, (2016).
[29] L. Zhang, L. Zhang, B. Du, Deep learning for remote sensing data: a technical tutorial on the state of the art, IEEE Geosci. Remote Sens. Mag. 4 (2) (2016) 22–40.
[30] Z. Gao, W. Gao, N. Bin Chang, Integrating temperature vegetation dryness index (TVDI) and regional water stress index (RWSI) for drought assessment with the aid of LANDSAT TM/ETM + images, Int. J. Appl. Earth Observ. Geoinf. 13 (3) (2011) 495–503.